Growth of textured aluminum films on $LiNbO_3$ piezoelectric substrate with ultrathin tantalum underlayer.

Hala Achahbar
frec|n|sys
Besancon, France
hala.achahbar@femto-st.fr

Florent Bernard
frec|n|sys
Besançon, France
florent.bernard@frecnsys.fr

Emilie Courjon
frec|n|sys
Besançon, France
emilie.courjon@frecnsys.fr

Thomas Baron
FEMTO-ST
Besançon, France
thomas.baron@femto-st.fr

Sylvain Balandras
frec|n|sys
Besançon, France
Sylvain.ballandras@frecnsys.fr

***Abstract*: In this paper the approach of improving aging of (AlCu2%) electrode of Surface acoustic Wave filters is presented. The goal of this study is to contribute of the improving of aging due to electromigration effect. This effect occur easily in high-frequency Surface Acoustic Wave (SAW) devices. For that purpose, the impact of a tantalum (Ta) thickness deposited between the electrodes (AlCu2%) and a piezoelectric $LiNbO_3$ is done. A heating post-process is also presented to increase the aging of such devices.**

Keywords: Piezoelectric, AlCu2% (111) texture, Ultrathin underlayer, Electromigration, $LiNbO_3$, SAW, Free surface energy, IDT,5G.

I. Introduction

In the context of 5G, Surface Acoustic Wave (SAW) filters have to increase their operating frequency. Thus, new technological challenges arise due to the reduction of the dimensions of the electrodes. One of them are the aging of electrodes which contribute to keeping filter characteristics. Most SAW filters are composed of AlCu2% electrodes deposited on a piezoelectric substrate such as Lithium Niobate ($LiNbO_3$) or Lithium Tantalate ($LiTaO_3$). Our work has to objective to keep AlCu2% electrode and improve the life time of such filters.

The life time of SAW-filters is limited by the degradation of the AlCu2% electrodes [1]. The degradation of AlCu2% electrodes are due to the migration of Al atoms along grain boundaries (GB). Which causes the formation of voids and hillock-like extrusion (see Figure 1). This phenomenon of migration is called electromigration (EM), which is the atomic displacement due to momentum transfer to metal atoms [2].

Several studies have found a promising and feasible approach to improve electromigration resistance by imposing a better crystallographic texture of that AlCu2% film [4,5,6,7] It was well demonstrated the AlCu2% electrodes with a highly texture (111) are more resistant to electromigration than those with poor (111) texture [4,5,6,7]

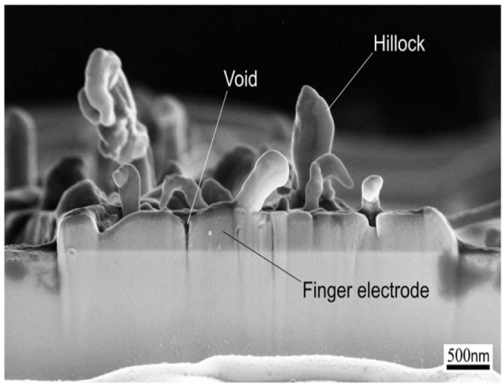

Figure 1: *SEM micrograph of a FIB cross section of a damaged Al finger electrode on $LiNbO_3$ (90° tilted) with strong hillock formation (after 2000 minutes at 3W) [2]*

Sulei Fu *et al.* report in a previous work [4] that the presence of ultrathin Ti underlayer between the substrate of $LiNbO_3$ and AlCu2% film can give a better textured AlCu2% film. It has also been reported by other authors that Ni or Zr as an underlayer provides an improvement in the (111) texture of the AlCu2% film [6][7]. However, Qi Li *et al.* [6] have demonstrated that the AlCu2% texture and structure quality decreases gradually as the underlayer thickness increases. Atsushi Kamijo and Tsutomu Mitsuzuka [5]

noted that a textured AlCu2% film can be obtained on a metal underlayer in a certain thickness range.

Therefore, to obtain fine-dimensional control in high-frequency SAW filters, one solution consists on improving the crystallographic texture and structure of the AlCu2% electrodes by using an ultrathin underlayer [4,5,6,7].

In this work, the presence of a tantalum (Ta) underlayer (with various thicknesses) on a 128-rotated Y-Cut $LiNbO_3$ substrate during AlCu2% film growth will be studied. Heat treatments of AlCu2% films to improve the crystallographic texture and structure of AlCu2% electrodes will also be investigated.

II. Growth modes

The mechanism of texturing can be explained by growing modes of the AlCu2% film on $LiNbO_3$ substrates. Theoretical models of thin films growth suggest that, one of the parameters that determine the growth model is the surface-interface energy balance between film and substrate (see Figure 2). allows to define the growth mode of the AlCu2% film as a Volmer-Weber or Frank-Van Der Merwe mode. This is represented by Young's equation (eq1) [8].

$$Cos\,(\theta) = \frac{(\gamma_s - \gamma_i)}{\gamma_f} \qquad (eq1)$$

where θ, γ_s, γ_i *and* γ_f *are* respectively the wetting angle of the island, substrate surface energy, film surface free energy, and interfacial free energy between film and substrate.

When the condition (eq2) is satisfied during the film deposition, the film is considered to develop at the Volmer–Weber growth mode (3D). In that case, the film grows randomly in the initial stage, resulting in poor texture [8].

$$\gamma_f + \gamma_i - \gamma_s > 0 \qquad (eq2)$$

In the Frank-Van Der Merwe growth mode, the condition changes to (eq3):

$$\gamma_f + \gamma_i - \gamma_s < 0 \qquad (eq3)$$

This mode is generally obtained when the substrate surface energy γ_s is higher than γ_f. The film grows by means of successive monolayers (see Figure 2), which favors the formation of a textured film [8].

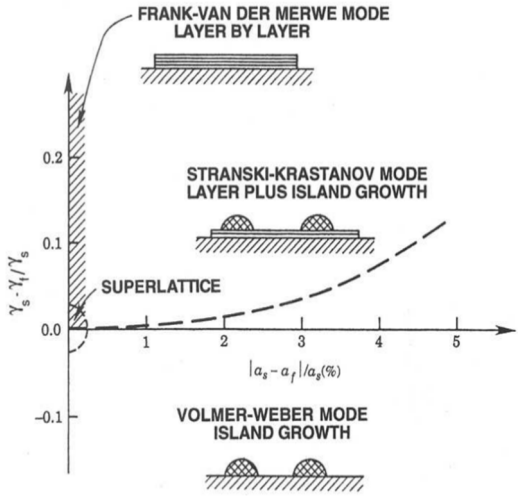

Figure2*: Stability regions of the growth modes versus surface energy between substrate and film and of lattice misfit [9]*

The work about surface energies of solids of Tu et *al.* [9] suggests that metals have higher surface energies than oxides, alkali halides, sulfides, and organic substances. The higher values correspond to the transition metals while the lower values is related to alkali and divalent metals.

Therefore, when AlCu2% film is deposited directly onto a $LiNbO_3$ substrate, the equation (2) is satisfied and the AlCu2% film grows randomly by the Volmer-Weber mode, which results in the formation of an AlCu2% polycrystalline film with poor texture [4,5,6,7].

The goal of this study is to increase the surface free energy (FSE) of the $LiNbO_3$ substrate by using an ultrathin underlayer (Ta) and then change the growth mode to improve the structure and the texture quality of AlCu2% electrodes

III. Experimentation

A. Film Deposition

A 100nm-thick AlCu2% film with several thicknesses of Ta underlayer (0, 1.3, 5 and 20 nm) has been deposited on 5 128°-rotated Y-Cut $LiNbO_3$ substrates (with a diameter of 4inches). Both films have been deposited by electron beam evaporation in a Balzers BAK760. Prior to layer deposition, substrates have been cleaned successively in Microposit Remover 1165 (50°C) and rinsed in deionized water for 10 min, then a short pre-clean with O_2 plasma was applied. Deposition of Ta underlayers was carried out with a rate of 0.3 $nm.s^{-1}$ at room temperature, after the chamber was evacuated down to 10^{-6} mbar by a combined vacuum system of mechanical pump and cryopump. Finally, without breaking vacuum, AlCu2% films were evaporated at a rate of 1 $nm.s^{-1}$ also. The thickness of both films was monitored by a quartz microbalance located inside the vacuum chamber. After deposition, a thermal treatment was carried out by heating the films (AlCu2%/Ta (1.3 nm)/$LiNbO_3$) in atmosphere at 1 °C/min to 523

and 623 K, holding at temperature for 3 hours before furnace cooling. Heat treatments have been performed in a AET tube furnace.

B. Characterizations

The crystalline structure of the films (100 nm-AlCu2%/$LiNbO_3$ and 100 nm-AlCu2%/1.3 nm-thick Ta/$LiNbO_3$) has been analyzed by diffractometer (XRD, SmartLab) in $\boldsymbol{\theta}$–$2\boldsymbol{\theta}$ scan and χ-scan (Cu(Kα) wavelength, λ = 0.154056 nm)).

To determine the FSE of a $LiNbO_3$ substrate with (0, 1.3, 5, and 20 nm) of Ta underlayer, contact angles of test liquids, whose FSE ($\boldsymbol{\gamma_l}$) including their dispersive $\boldsymbol{\gamma_l^d}$ and polar $\boldsymbol{\gamma_l^p}$ parts are known [13], are measured. Contact angles $\boldsymbol{\theta}$ have been measured by static sessile drop method using a Digidrop – MCAT Goniometer (GBX). The device used for contact angle measurement includes a holder with microliter syringe. Drops are backlighted by LEDs. Evaluation of contact angles from the camera data has been performed on a Visiodrop software. Test liquids were chosen in this study are Formamide (99%), ethylene glycol (99.8%) glycerol (99%) deionized (DI) water, and 50% ethylene glycol +50% DI water (purchased from VWR-Chemicals). The selection of these liquids was based on the following criteria:

1. liquid should not react with substrate;
2. liquids should be non-toxic;
3. the liquid surface tension should be higher than the anticipated solid surface tension [10][11].

The dispersive and polar parts of liquids surface tension are used to calculate FSE of substrates ($\boldsymbol{\gamma_s}$) based on a mathematical model. This model, knows as Owens-Wendt model [12], considers the geometric mean of the dispersive and polar parts of the liquids surface tension and of the solids FSE (eq4) [12]:

$$\boldsymbol{\gamma_{sl} = \gamma_s + \gamma_l - 2\sqrt{\gamma_s^d \gamma_l^d} - 2\sqrt{\gamma_s^p \gamma_l^p}} \qquad \textit{(eq4)}$$

Substituting this expression in the Young equation: $\gamma_s = \gamma_{sl} + \gamma_l \cos(\theta)$ a linear equation of the type $y = ax + b$ can be obtained [12]:

$$\frac{\boldsymbol{\gamma_l(1+Cos(\theta))}}{\boldsymbol{2\sqrt{\gamma_l^d}}} = \boldsymbol{\sqrt{\gamma_s^p}\sqrt{\frac{\gamma_l^p}{\gamma_l^d}} + \sqrt{\gamma_s^d}} \qquad \textit{(eq5)}$$

These equations $\boldsymbol{y = \frac{\gamma_l(1+Cos(\theta))}{2\sqrt{\gamma_l^d}}}$ and $\boldsymbol{x = \sqrt{\frac{\gamma_l^p}{\gamma_l^d}}}$ contain the known quantities, namely the measured contact angle $\boldsymbol{\theta}$ and the dispersive $\boldsymbol{\gamma_l^d}$ and polar $\boldsymbol{\gamma_l^p}$ parts of the test liquid's surface tension. The searched dispersive and polar parts of the solids FSE are contained in the axis intercept b and in the slope a, respectively. The regression leads directly to the components of the solid: $\boldsymbol{\gamma_s^p = a^2}$; $\boldsymbol{\gamma_s^d = b^2}$

$$\boldsymbol{\gamma_s = \gamma_s^p + \gamma_s^d} \qquad \textit{(eq6)}$$

IV. Results and discussion

A. Free surface energy

Firstly, we must note, that the results obtained in this study are qualitative. The goal is to follow the evolution of the FSE of $LiNbO_3$ as a function of Ta underlayer thickness (1.3, 5,20 nm).

The abscissa ($\boldsymbol{y = \frac{\gamma_l(1+Cos(\theta))}{2\sqrt{\gamma_l^d}}}$) and ordinate $\boldsymbol{x = \sqrt{\gamma_l^p/\gamma_l^d}}$ pairs are calculated for each measurement.

Table 1 represents the FSE values obtained by the Owens-Wendt method for $LiNbO_3$ wafers and for 5 nm-thick, 20 nm thick and 1.3 nm-thick Ta films deposited on $LiNbO_3$ wafers.

Table1 *Calculated FSE* values using Owens-Wendt method for substrates (all in mJ.m^{-2})

Substrates	LiNbO3	5nm-thick Ta / LiNbO3	20nm-thick Ta / LiNbO3	1.3nm-thick Ta / LiNbO3
$\gamma_s^d = b^2$	17,64	20,95	22,75	21,40
$\gamma_s^p = a^2$	29,45	26,83	23,67	28,69
γ_s	47,09	47,79	46,43	50,10
FSE mJ/m²	**47,09 ± 1,07**	**47,79 ± 0,78**	**46,43 ± 0,99**	**50,10 ± 1,34**

The value of the substrate FSE ($\boldsymbol{\gamma_s}$) calculated by the Owens method increases in the presence of 1.3nm of Ta, $\boldsymbol{\gamma_s}$ is equal to 50.10 ± 1.34 mJ/m². Moreover, the FSE value decreases from 47.79 ± 0.78 mJ/m² to 46.43 ± 0.99 mJ/m² when the thickness changes from 5 nm to 20 nm of Ta (see Figure 2).

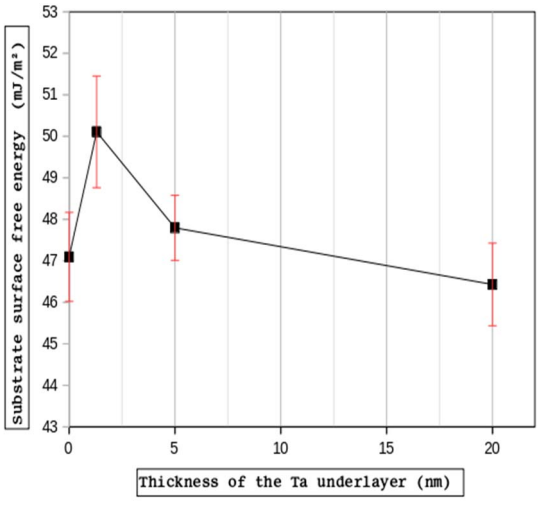

Figure 3: *Evolution of the free FSE of $LiNbO_3$ as a function of the thickness of Ta.*

These results confirm the advantage of using an

ultrathin underlayer of Ta (<5 nm) to increases the FSE of the $LiNbO_3$ substrate. This high surface free energy comes from the fine grains of Ta dispersed on the $LiNbO_3$ surface. It is assumed that the 1.3 nm-thick Ta underlay is the best candidate that will allow the γ_s to increase and therefore promote a switch from Volmer-Weber mode (eq2) to the Frank-Van Der Merwe mode (eq3). Then will allow the AlCu2% film to grow layer by layer with fewer grain boundaries and a single preferred orientation.

B. Crystal structures quality

In order to characterize the AlCu2% (111) texture X-Ray Diffraction was employed. XRD are carried out on the $LiNbO_3$ bare surface and $LiNbO_3$ with 100 nm-thick AlCu2% film (see Figure. 4).

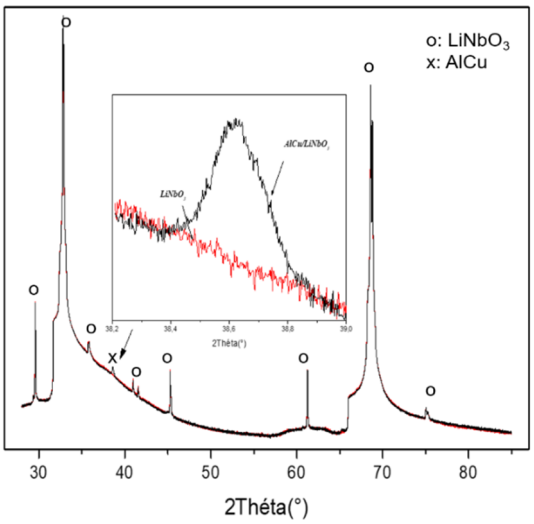

Figure 4*: XRD patterns of θ-2θ scans of AlCu2% electrodes*

We can clearly see that only one Bragg peak appears at 2**θ** of 38° (Figure 4), which corresponds to the Al (111), in the range of 30°–80°. The apparent presence of only Al (111) without other peaks demonstrates that (111) preferred AlCu2% thin films are developed on 128°-rotated-Cut- $LiNbO_3$.

When inserting an ultrathin Ta underlayer (1.3 nm) between the $LiNbO_3$ substrate and the AlCu2% film the AlCu2% (111) peak remains the same (see Figure 5).

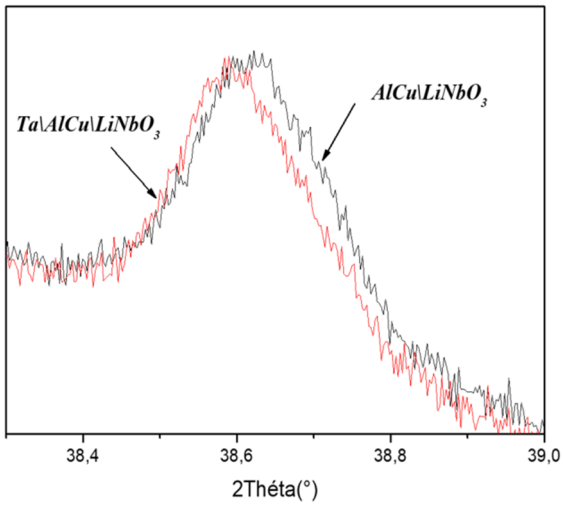

Figure 5: Evolution of the peak AlCu2% (111) in the presence of the Ta underlayer.

The microstructure of AlCu2% thin films grown on Ta (1.3 nm)/$LiNbO_3$ is stabilized by an annealing step in atmosphere at (523 and 623 K) (see Figure 6).

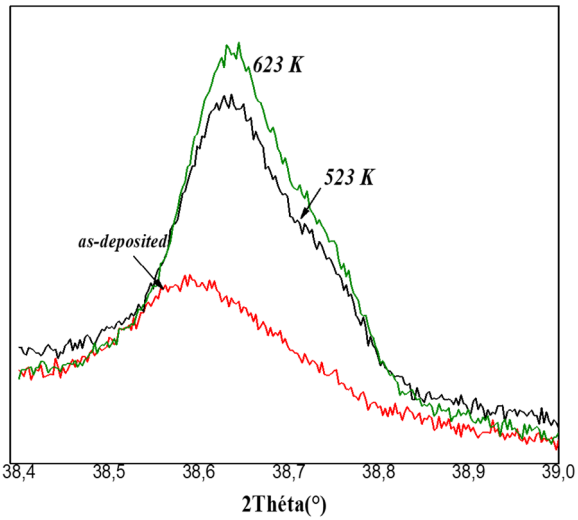

Figure 6: *Evolution of the peak (111) as a function of the annealing temperature for the 100 nm AlCu2% film deposited on a 1.3 nm underlay of Ta*

On figure 7, we can see that the full width at half maximum (FWHM) value decreases after heat treatment.

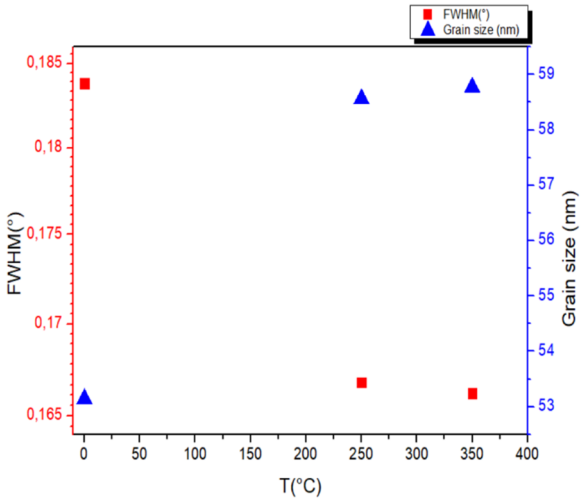

Figure 7: *Evolution of the FWHM and grain size of AlCu2% films as a function of the annealing temperatures*

The grain size value is 53 nm for samples as-deposited but raises to 58 nm and to 58 nm when the annealing temperature increases to 523 K and 623 K.

At this stage of the study, an improvement in the structure and crystalline quality of the AlCu2% films with 1.3 nm-thick Ta underlayer and annealing was observed. Other XRD analysis of AlCu2% films with Ta underlayer (5 nm and 20 nm) are in progress. Further studies of stress in AlCu2% films without Ta underlayer and with a Ta underlayer lower than 10 nm are ongoing in order to determine the effect of the Ta underlayer in lattice mismatch and strain between the AlCu2% film and the $LiNbO_3$ substrate and therefore confirm if the Ta ultrathin layer can really allow AlCu films to grow in Frank-van der Merwe mode.

v. Conclusion

A series of AlCu2% films with different Ta underlayer thicknesses has been deposited on $LiNbO_3$ wafers by electron beam evaporation. Contact angle measurement show that the presence of 1.3 nm-thick Ta underlayer onto $LiNbO_3$ surface can greatly increases the surface free energy of the $LiNbO_3$ substrate. The 1.3nm-Ta/AlCu2%/$LiNbO_3$ seems to be the best configuration to privilege the Frank-van der Merwe mode.

The XRD studies showed that 1.3-nm Ta underlayer and a heat treatment (523-623 K) improves the texture and crystalline quality of AlCu2%. Hence, reduce the diffusion of Al atoms into GB, and subsequently improve the resistant to electromigration phenomenon.

Abbreviations and Acronyms

SAW: Surface Acoustic Wave
EM: Electromigration
IDT: Interdigital transducer
FSE: Free surface energy
FWHM: Full width at half maximum
XRD: X-ray diffraction
AlCu2%: Alloy aluminum copper 2%.

Acknowledgements

The authors are grateful to Dr. Ausrine Bartasyte (Time & Frequency department, FEMTO-ST) and her team for XRD characterizations.
We would also thank our colleagues from the technology center of FEMTO-ST, MIMENTO for their support.
This work was partly supported by the french RENATECH network and its FEMTO-ST technological facility.
This work was partly supported by the french First-TF network project.
We would like to thank the EUR EIPHI program for the project financial support (Contract No. ANR17-EURE-0002)

REFERENCES

[1] Christoph Eberl," Fatigue of Al Thin Films at Ultra High Frequencies" thesis, Universität Stuttgart, 2005.
[2] L. Arnaud, T. Berger, G. Reimbold, Evidence of grain-boundary versus interface diffusion in electromigration experiments in copper damascene interconnects, J. Appl. Phys. 93 (1) (2003) 192–204. l
[3] M. Pekarcikova, M. Hofmann, S. Menzel, H. Schrnidt, T. Gemming and K. Wetzig, "Investigation of high power effects on Ti/Al and Ta-Si-N/Cu/Ta-Si-N electrodes for SAW devices," in IEEE Transactions on Ultrasonics, Ferroelectrics, and Frequency Control, vol. 52, no. 5, pp. 911-917, May 2005, doi: 10.1109/TUFFC.2005.1503977
[4] Sulei Fu, Weibiao Wang, Li Xiao, Zengtian Lu, Qi Li, Cheng Song, Fei Zeng, and Feng Pan, Texture- enhanced Al-Cu electrodes on ultrathin Ti buffer layers for high-power durable 2.6 GHz SAW filters,American Institute of Physics.
[5] Atsushi Kamijo and Tsutomu Mitsuzuka, A highly oriented {Al}[111] texture developed on ultrathin metal underlayers, Journal of Applied Physics.
[6] Qi Li, Su-Lei Fu, Cheng Song, Guang-Yue Wang, Fei Zeng, Improved resistance to electromigration and acoustomigration of Al interdigital transducers by Ni underlayer, Springer Nature.
[7] D. M. Li, F. Pan, X.B.Wang, J.B.Niu, M.Liu, Microstructure and Electronic Properties of Al/Zr/LiNbO 3Multilayers, Materials Science Forum.
[8] Ohring Milton, The Materials Science of Thin Films, San Diego New York Boston (Mass.), 1992.
[9] K.-N, Tu, J. W. Mayer, and L. C. Feldman, Electronic Thin Film NScience for Electrical Engineers and Materials Scientists. Macmillan, New York, 1992
[10] W.A. Zisman, Contact angle, wettability and adhesion, in: Advances in Chemistry Series, vol. 43, American Chemical Society, Washington, DC, 1964.
[11] F.M. Fowkes, Ind. Eng. Chem. 12 _1964. 40.
[12] Owens D.K., Wendt R.C. Estimation of the surface free energy of polymers. J Appl. Polym. doi: 10.1002/app.1969.070130815
[13] http://www.accudynetest.com/surface_tension_table.htm